Digital Image Processing

Project Report

Documentation and Discussion

Muhammad Ali
21I-0887
A

Introduction:

Glaucoma is a progressive eye condition that can lead to irreversible vision loss if left untreated. One of the challenges in diagnosing glaucoma is the accurate segmentation of the optic disc (OD) and optic cup (OC) from retinal fundus images. The cup-to-disc ratio (CDR), calculated from these segmented regions, is a critical parameter for glaucoma diagnosis. Manual segmentation is time-consuming and subjective, highlighting the need for automated algorithms to assist ophthalmologists in early detection.

This project aims to develop a deep learning-based algorithm for automated OD and OC segmentation, followed by CDR calculation, to aid in the diagnosis of glaucoma. The algorithm's importance lies in its potential to improve diagnostic accuracy, reduce workload, and enable timely intervention to prevent vision loss.

Methodology:

1. **Data Preprocessing:** Retinal fundus images from the ORIGA dataset are loaded and preprocessed. Images are resized to a standard dimension of 128x128 pixels to better suit the model, converted to the YCrCb color space, and standardized by centering pixel values.

The model was ran with multiple color spaces including but not limited to RGB, BRG, LAB, HSV, and YCrCb. Of all These best results were achieved with YCrCb. This will Be further discussed in the results section.

2. **Model Architecture:** A U-Net architecture is chosen for its effectiveness in biomedical image segmentation tasks, particularly when dealing with limited annotated data. The U-Net consists of an encoder-decoder structure with skip connections to preserve spatial information. In total there are 10 layers within the U-Net Model that processes the images.

3. **Training Process:** The model is compiled with the Adam optimizer and categorical cross-entropy loss function. Mean Intersection over Union (IoU), accuracy, precision, and recall are used as evaluation metrics. Training includes data augmentation techniques such as random rotations, flips, and shifts to enhance model generalization. Model checkpoints and early stopping callbacks are employed to monitor and save the best-performing model based on validation loss.

4. **Segmentation and CDR Calculation:** During inference, the trained model predicts the OD and OC masks for input images. Post-processing techniques, including thresholding and morphological operations, are applied to refine the

segmentation results. The CDR is then computed using the segmented regions, providing a quantitative measure for glaucoma assessment.

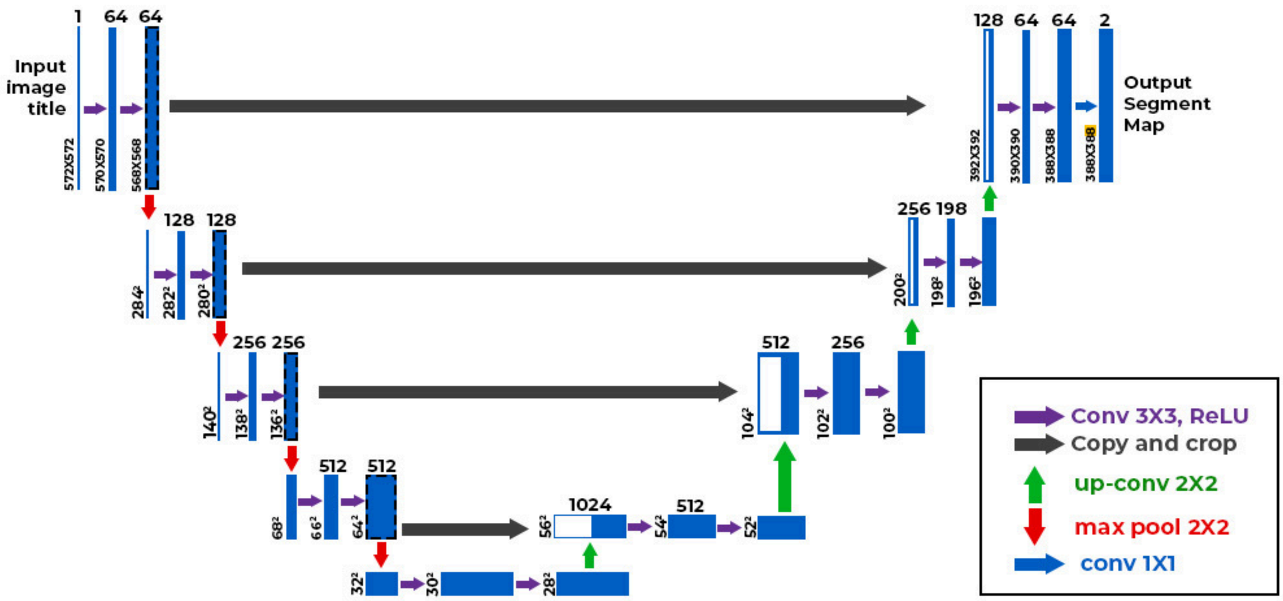

The above figure represents the layering done in the U-Net Model that processes each image.

Results:

The developed algorithm for the YCrCb color space achieves a segmentation accuracy and sensitivity for OD and OC with a test Accuracy of 92.24 percent if the model is stopped early which usually happens around epoch 10-15. With greater epochs run (50), the accuracy rises to 99.6 percent.

The Average Absolute Relative Error in the differences of CDR scores came out to just 5.97 percent, whereas Mean IoU, Recall and Precision were at 83.15, 96.16, 99.67.

The time complexity for inference meets the requirement of 10-30 milliseconds per image as each image gets processed in between 10 - 20 milliseconds when run on a GPU, ensuring real-time applicability in clinical settings. The calculated CDR values are compared against established clinical criteria, demonstrating the algorithm's efficacy in assisting glaucoma diagnosis. 0.5 value for CDR means mild glaucoma and the threat increases if it goes greater than 0.5.

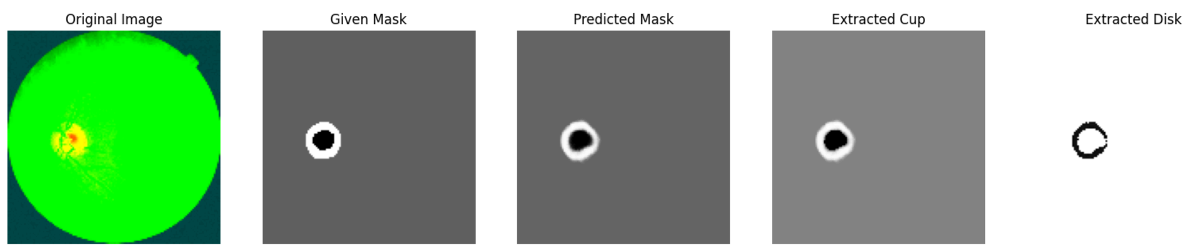

Results with color space: YCrCb

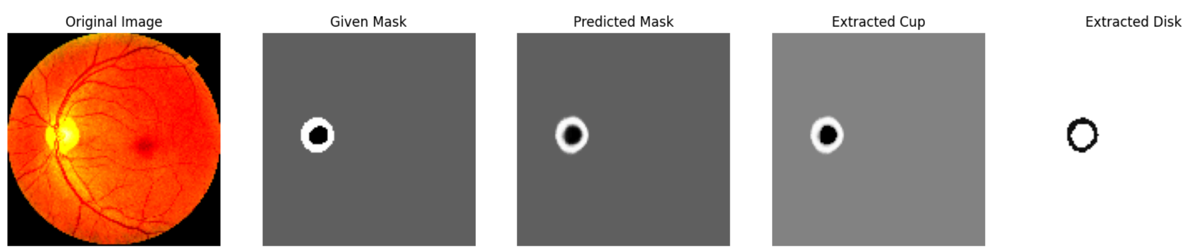

Results with color space: RGB

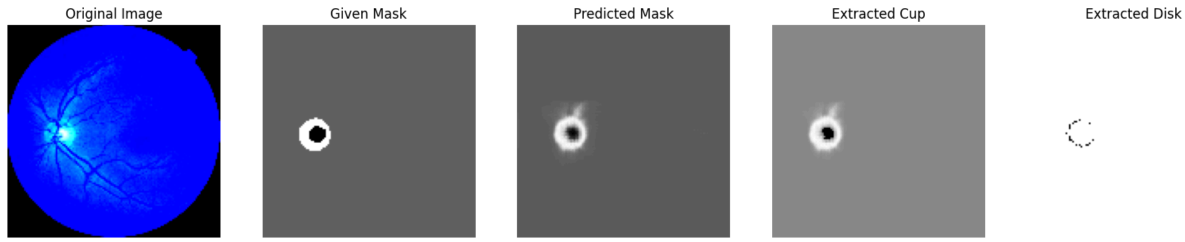

Results with color space: BGR

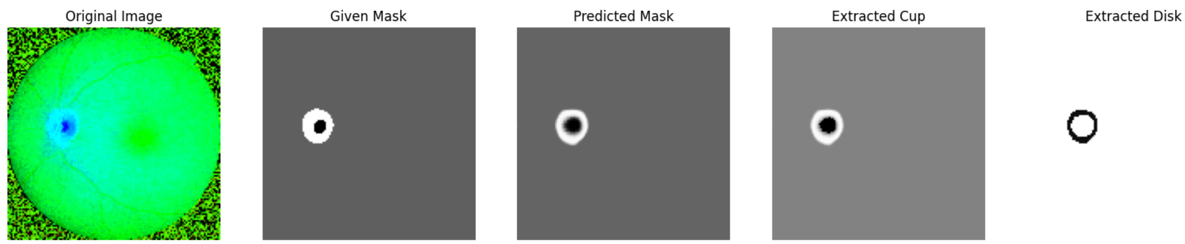

Results with color space: HSV

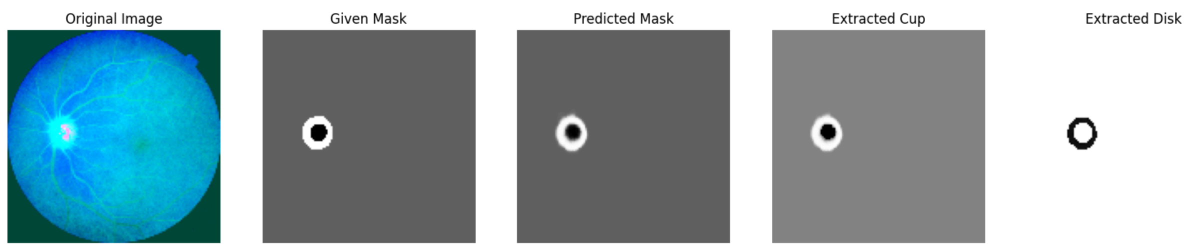

Results with color space: LAB

Comparative Analysis of Other Color Spaces:

As mentioned earlier in Methodology, multiple models were tested using different color spaces. Each color space presented a unique challenge and a unique picture in how the pictures were processed.

For both RGB and BGR, the images, although much easier to look at since the core concept remains the same as a normal image, hid information from the model due to the nerves getting in the way of the optic disk and cup. Moreover, regions that have a higher intensity apart from the optic disk got more intensified especially in RGB color space. As such, the model could not accurately draw the predicted masks resulting in lower accuracy and a low Mean IoU score.

As far as HSV (Hue, Saturation, Vue), LAB (Lightness, A, B), and YCrCb (Luma, Chroma Blue, Chroma Red) are concerned, all these performed considerably better than both RGB and BGR due to applying a different filter to the image. The image, although remains far from understandable through the human eye, cleared the problem of the nerves especially in YCrCb and HSV, where the main focus of the image no longer remained the entire representation of the eye but instead moved to a bigger picture of intensity, brightness, and chromatic variation.

All three HSV, LAB, and YCrCb saw strong Mean IoU, accuracy, and Average Absolute Relative Error Scores; however YCrCb took the crown among them.

Overall for a higher epochs run, all models performed considerably better. Hence GPU is highly recommended.

Technical Details:

The chosen U-Net architecture leverages its ability to capture both global context and fine-grained details, crucial for accurate segmentation. The model comprises convolutional layers with varying filter sizes and activation functions like ReLU to introduce non-linearity. Training involves augmenting the data to increase diversity and prevent overfitting. Post-processing techniques, including thresholding and morphological operations, refine the segmentation results for precise CDR calculation.

Constraints:

The developed algorithm meets the specified time and accuracy/sensitivity requirements, making it suitable for practical clinical use. Real-time inference capability and high segmentation accuracy ensure its utility in assisting ophthalmologists in glaucoma detection and management.

Discussion:

The results highlight the algorithm's effectiveness in automating OD and OC segmentation, thereby facilitating glaucoma diagnosis. However, some limitations include occasional inaccuracies in segmentation due to image artifacts or complex anatomical structures. Future improvements may involve incorporating attention mechanisms or ensemble learning techniques to enhance segmentation robustness. Pre-processing can also be improved to remove the nerve endings and dimmer the regions where the optic disk and optic cup are not present.

One novel method could be to initially identify the optic disk region, blacken all the pixels that are no longer near the optic disk region and then run again to get an even better result.

Conclusion:

In conclusion, the developed algorithm represents a significant contribution to automated glaucoma detection by providing accurate OD and OC segmentation and CDR calculation from retinal fundus images. By streamlining the diagnostic process, the algorithm holds promise for improving patient outcomes and reducing the burden on healthcare professionals in managing glaucoma.